

Thermogravimetric analysis-mass spectrometry (TGA-MS) of hydrotalcites containing CO_3^{2-} , NO_3^- , Cl^- , SO_4^{2-} or ClO_4^-

J. Theo Kloprogge^a, János Kristóf^b and Ray L. Frost^a

^a Centre for Instrumental and Developmental Chemistry, Queensland University of Technology, 2 George Street, GPO Box 2434, Brisbane, Qld 4001, Australia.

^b Department of Analytical Chemistry, University of Veszprém, H8201 Veszprém, P.O. Box 158, Hungary.

In 2001. A Clay Odyssey. Proceedings of the 12th International Clay Conference Bahai-Blanca, Argentina, July 22-28, 2001, Dominguez, E., Mas, G. and Cravero, F. (editors), ISBN 0-444-50945-3.

Mg/Al-hydrotalcites containing NO_3^- , Cl^- , SO_4^{2-} or ClO_4^- were synthesised under N_2 to prevent incorporation of CO_3^{2-} . The presence of the anions in the hydrotalcite structure was confirmed by infrared and Raman spectroscopy. The CO_3 - and the NO_3 -hydrotalcites contained both NO_3^- and CO_3^{2-} , while the Cl-hydrotalcite also contained some CO_3^{2-} . It is known that during thermal treatment of hydrotalcites dehydroxylation and decarbonisation strongly overlap. Mass spectrometry following TGA enables one to identify both reactions. For CO_3 -hydrotalcite CO_2 is released simultaneously with water (dehydroxylation) around 335°C followed by NO around 365 and 500°C . The stability of the NO_3 -hydrotalcite is different showing a major loss of CO_2 and H_2O (dehydroxylation) around 410°C with losses of NO around 345 and 450°C . The Cl-hydrotalcite shows a similar behaviour for the H_2O loss (dehydroxylation), but Cl is lost over a range from 400 to 900°C and CO_2 comes off in steps around 360 and 500°C . Completely different is the thermal behaviour of SO_4 - and ClO_4 -hydrotalcites. SO_4 -hydrotalcite shows a gradual weight-loss due to dehydroxylation with two minor water peaks around 260 and 375°C , while the sulphate remains in the structure. The sulphate is not lost until heated to 900°C . The ClO_4 -hydrotalcite shows a complex thermal behaviour with 2 steps of water loss around 375 and 440°C , where the second step is accompanied by the loss of O_2 . A possible explanation is a redox reaction between perchlorate and the cations giving metal-chlorides and O_2 .

1. INTRODUCTION

Layered double hydroxides (LDHs) are also known as hydrotalcites or anionic clays, due to their layered structure with a charge opposite to that of smectites. The structure of hydrotalcite can be visualised as positively charged OH-layers comparable to those in brucite ($\text{Mg}(\text{OH})_2$) in which a part of the Mg^{2+} is substituted by a trivalent metal such as Al^{3+} separated by charge compensating, mostly hydrated, anions between the hydroxide sheets. In layered double hydroxides a large range of compositions is possible based on a general formula of $[\text{M}^{2+}_{1-x}\text{M}^{3+}_x(\text{OH})_2][\text{A}^{n-}]_{x/n}\cdot y\text{H}_2\text{O}$, where M^{2+} and M^{3+} are the di- and trivalent metals in the octahedral sites within the OH-sheets with x normally between 0.17 and 0.33 .

The number of anions or anionic complexes in layered double hydroxides is essentially unlimited provided that the anion does not form a complex with the cations in the hydroxide sheets during the formation (Vaccari 1998). Therefore, the variety possible in both the cationic and anionic compositions of the hydrotalcite offers the possibility to prepare tailor-made materials for specific applications, such as basic catalysts, as a precursor for the preparation of mixed metal oxidic catalysts, absorbents, as for other specific powder properties such as filler, UV-radiation stabiliser, chloride scavenger and thermal stabiliser (Titulaer 1993).

In some recent publications (Kloprogge et al., 2000, 2002) we have described the incorporation of CO_3^{2-} , NO_3^- , SO_4^{2-} and ClO_4^- in hydrotalcites and the effects that the confinement of these anions in the interlayer space of hydrotalcites has on their vibrational spectra (infrared and Raman) in comparison to the anions in solution. It was shown that in comparison to free CO_3^{2-} a shift towards lower wavenumbers was observed. A band around $3000\text{-}3200\text{ cm}^{-1}$ has been attributed to the bridging mode $\text{H}_2\text{O-CO}_3^{2-}$. The IR spectrum of the CO_3 -hydrotalcite clearly shows the split ν_3 around 1365 and 1400 cm^{-1} together with weak ν_2 and ν_4 modes around 870 and 667 cm^{-1} . The ν_1 is activated and observed as a weak band around 1012 cm^{-1} . The Raman spectrum shows a strong ν_1 at 1053 cm^{-1} plus weak ν_3 and ν_4 modes around 1403 and 695 cm^{-1} . The symmetry of the carbonate anions is lowered from D_{3h} to C_{2v} resulting in activation of the IR inactive ν_1 mode around $1050\text{-}1060\text{ cm}^{-1}$. In addition, the ν_3 shows a splitting of $30\text{-}60\text{ cm}^{-1}$. Although the NO_3 -hydrotalcite has incorporated some CO_3^{2-} the IR shows a strong ν_3 at 1360 cm^{-1} with a weak band at 827 cm^{-1} , ν_4 is observed at 667 cm^{-1} , although it is largely obscured by the hydrotalcite lattice modes. The Raman spectrum shows a strong ν_1 at 1044 cm^{-1} with a weaker ν_4 at 712 cm^{-1} . The ν_3 at 1355 cm^{-1} is obscured by a broad band due to the presence of CO_3^{2-} . The symmetry of NO_3^- did not change when incorporated in the hydrotalcite. The IR spectrum of the SO_4 -hydrotalcite shows a strong ν_3 at 1126 , ν_4 at 614 and a weak ν_1 at 981 cm^{-1} . The Raman spectrum is characterised by a strong ν_1 at 982 cm^{-1} plus medium ν_2 and ν_4 at 453 and 611 cm^{-1} , ν_3 can not be identified as a separate band, although a broad band can be seen around 1134 cm^{-1} . The site symmetry of SO_4^{2-} is lowered from T_d to C_{2v} . The distortion of ClO_4^- in the interlayer of hydrotalcite is reflected in the IR spectrum with both ν_3 and ν_4 split around $1096 + 1145\text{ cm}^{-1}$ and $626 + 635\text{ cm}^{-1}$, respectively. A weak ν_1 is observed at 935 cm^{-1} . The Raman spectrum shows a strong ν_1 around 936 cm^{-1} plus ν_2 and ν_4 at 461 and 626 cm^{-1} , respectively. ν_3 cannot be clearly recognised, but a broad band is visible around 1110 cm^{-1} . These data indicative a symmetry lowering from T_d to C_s .

In this paper we describe the thermal behaviour of these hydrotalcites containing CO_3^{2-} , NO_3^- , SO_4^{2-} and ClO_4^- . In addition to the weight losses as function of temperature as measured with conventional thermogravimetric analysis and differential thermal analysis, the evolved gasses were analysed by mass spectrometry. This way it is possible to get a better understanding of the mechanisms involved in the decomposition of hydrotalcites containing various anions.

2. EXPERIMENTAL METHODS

2.1 Synthesis of the Mg/Al-hydrotalcites containing CO_3^{2-} , NO_3^- , Cl^- , SO_4^{2-} and ClO_4^-

The hydrotalcite with theoretical composition of $\text{Mg}_6\text{Al}_2(\text{OH})_{16}\text{CO}_3 \cdot n\text{H}_2\text{O}$ was synthesised according to the method described before by Kloprogge and Frost (1999). This method comprises the slow simultaneous addition of a mixed aluminium nitrate (0.25M)-magnesium nitrate (0.75M) and a mixed NaOH (2.00M)- Na_2CO_3 (0.125M) solution under vigorous stirring buffering the pH at approximately 10. The product was washed to eliminate excess salt and dried at 60°C.

The incorporation of carbonate during the synthesis of the hydrotalcites containing the other anions was as much as possible prevented by boiling the deionised water before use, by rinsing the NaOH pellets before use and by executing the synthesis under a nitrogen atmosphere. As sources for the sulphate and perchlorate anions in solution the corresponding magnesium and aluminium salts were used instead of the magnesium and aluminium nitrates as discussed above.

The crystalline nature of the resulting materials was checked by X-ray powder diffraction (XRD). The XRD analyses were carried out on a Philips wide angle PW 1050/25 vertical goniometer equipped with a graphite diffracted beam monochromator. The radiation applied was $\text{CoK}\alpha$ (1.7902 Å) from a long fine focus Co tube operating at 35 kV and 40 mA. The samples were measured at 50 % relative humidity in stepscan mode with steps of $0.02^\circ 2\theta$ and a counting time of 2s.

2.2. Analytical techniques

Thermoanalytical investigations were carried out in a Netzsch (Selb, Germany) TG 209 type thermobalance in a flowing argon atmosphere of 99.995% purity (Messer Griesheim, Hungary) at a heating rate of 10°C/min. To simultaneously follow the evolution of the gaseous decomposition products over the temperature range investigated, the thermobalance was connected to a Balzers MSC 200 Thermo-Cube type mass spectrometer (Balzers AG, Lichtenstein). The transfer line to introduce gaseous decomposition products into the mass spectrometer was a deactivated fused silica capillary (Infochroma AG, Zug, Switzerland; 0.23 mm o.d.) temperature controlled to 150°C to avoid possible condensation of the evolved gases. In this way the thermogravimetric (TG), derivative thermogravimetric (DTG) and mass spectrometric ion intensity curves of the selected ionic species could be recorded simultaneously.

The finely powdered samples were combined with oven dried spectroscopic grade KBr (containing approximately 1 wt% sample) and pressed into a disc under vacuum. The spectra were recorded in triplicate by accumulating 512 scans at 4 cm^{-1} resolution in the spectral range between 400 cm^{-1} and 4000 cm^{-1} using the Perkin-Elmer 1600 series Fourier transform infrared spectrometer equipped with a LITA detector and on a Nicolet Magna 750 Fourier transform infrared spectrometer equipped with a DTGS detector. The Fourier transform Raman spectroscopic (FT-Raman) analyses were performed on a Perkin Elmer System 2000 Fourier transform spectrometer equipped with a Raman accessory comprising a Spectron Laser Systems SL301 Nd:YAG laser operating a wavelength of 1064 nm. 1000 scans were obtained at a spectral resolution of 4 cm^{-1} in order to obtain an acceptable signal/noise ratio.

3. RESULTS AND DISCUSSION

3.1. Characterisation of the solid materials

All the samples synthesised for this study were identified as Mg/Al-hydroxycalcites. Fig. 1 shows the XRD patterns of the synthesised hydroxycalcites. The hydroxycalcites synthesised with carbonate, nitrate or sulphate as the interlayer anion clearly show one crystalline phase. The value of 7.8 Å is characteristic of the 003 reflection of carbonate containing hydroxycalcite (Fig. 1) Replacement of carbonate by nitrate as the interlayer anion results in a slight expansion from 7.8 Å to around 8.1 Å, which is slightly smaller compared to the value of 8.36 Å reported by Marino and Masculo (1982). Incorporation of sulphate gives a 003 reflection of 8.9 Å that agrees well with data reported by e.g. Miyata and Okada (1977), Bish (1980) and Sato et al. (1986). The sample with the perchlorate as the interlayer anion however clearly shows a second phase with a 003 reflection similar to that of a carbonate containing hydroxycalcite in addition to a stronger reflection at 9.3 Å, which agrees with data reported by Miyata and Kumura (1973) and Brindley and Kikkawa (1980). A similar observation of two separate phases containing perchlorate and carbonate was made by Brindley and Kikkawa (1979).

Infrared spectroscopy (Fig. 2) was used at this stage to identify the interlayer anions in the hydroxycalcites synthesised. This confirmed clearly the presence of carbonate in the perchlorate system. So, even though greatest care was taken to exclude carbonate from the system, carbonate is sometimes found in the interlayer space. A similar observation was made in the infrared spectra of the nitrate containing hydroxycalcite, which probably also explains the slightly smaller 003 value and the broadening of the reflection compared to that of the carbonate containing hydroxycalcite. Opposite to these observations, the use of nitrate salts in the case of the carbonate containing hydroxycalcite resulted in the incorporation of a minor amount of nitrate as well, as was earlier observed by Klopogge and coworkers. (Hickey et al. 2000, Klopogge et al. 2000).

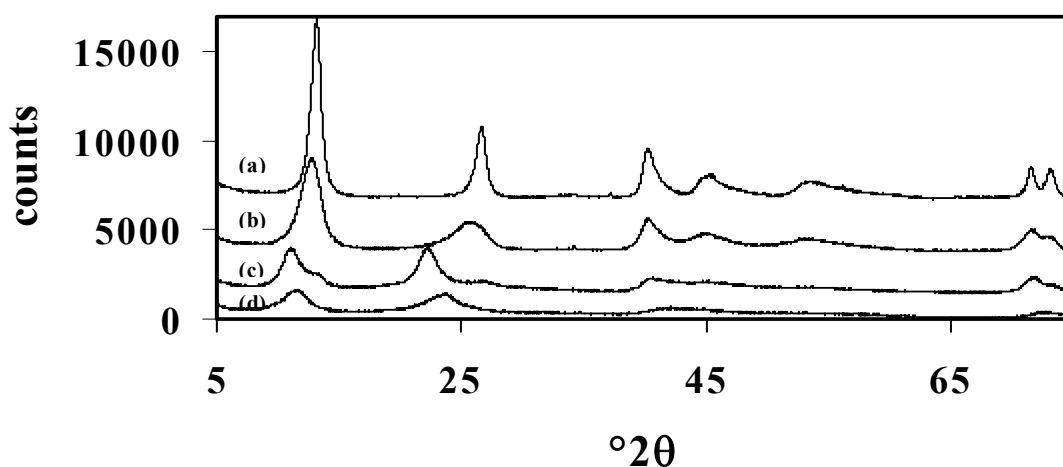


Fig. 1 XRD patterns of the hydroxycalcites containing (a) CO_3^{2-} , (b) NO_3^- , (c) ClO_4^{2-} and (d) SO_4^{2-} .

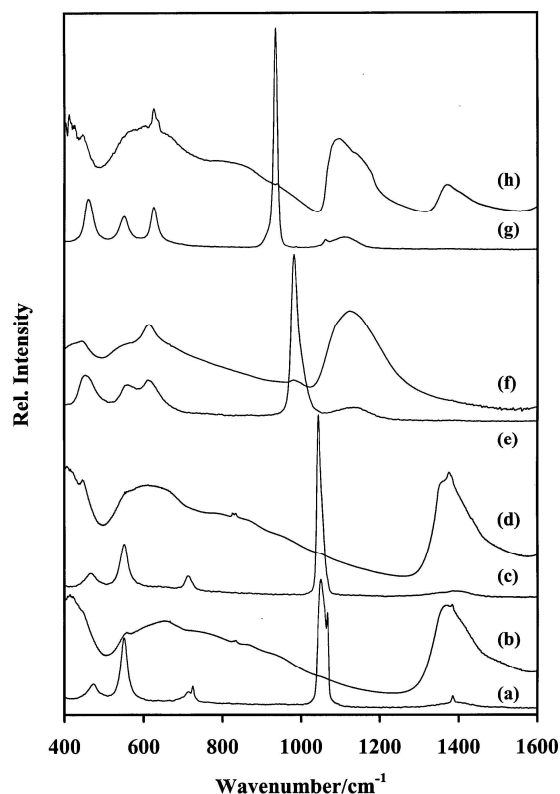


Fig. 2 Spectra of hydrotalcite containing CO_3^{2-} (a) Raman, (b) IR; NO_3^- (c) Raman, (d) IR; SO_4^{2-} (e) Raman, (f) IR and ClO_4^- (g) Raman and (h) IR.

3.2. Thermal behaviour of the anions in hydrotalcite

All the TGA patterns of the hydrotalcites, containing various anions, are characterized by a weight loss between 10 and 20 wt% due to loss of interlayer water with a maximum around 75-115°C. For CO_3 -hydrotalcite (Fig. 3) The dehydration takes place in two minor steps followed by a larger step around 197°C. These steps can be interpreted as being due to the loss of adsorbed water followed by loosely bound interlayer water and finally water coordinated to the interlayer carbonate.

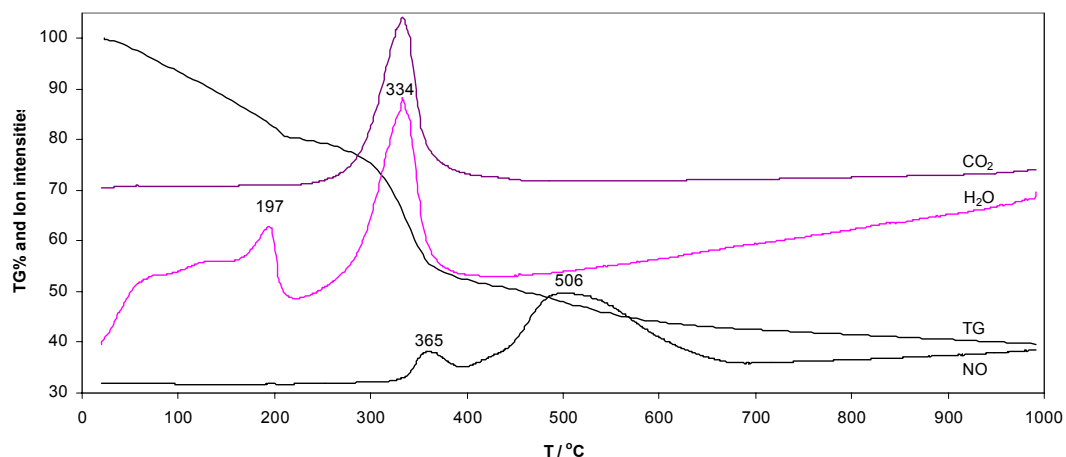


Fig. 3. TGA-MS patterns of CO_3 -hydrotalcite.

The three steps of dehydration are also observed in the corresponding differential thermal analysis pattern. The interlayer carbonate is released as CO_2 simultaneously with water around 335°C followed by NO around 365 and 500°C . This water loss around 335°C is due to the dehydroxylation of the Mg/Al -hydroxide sheets.

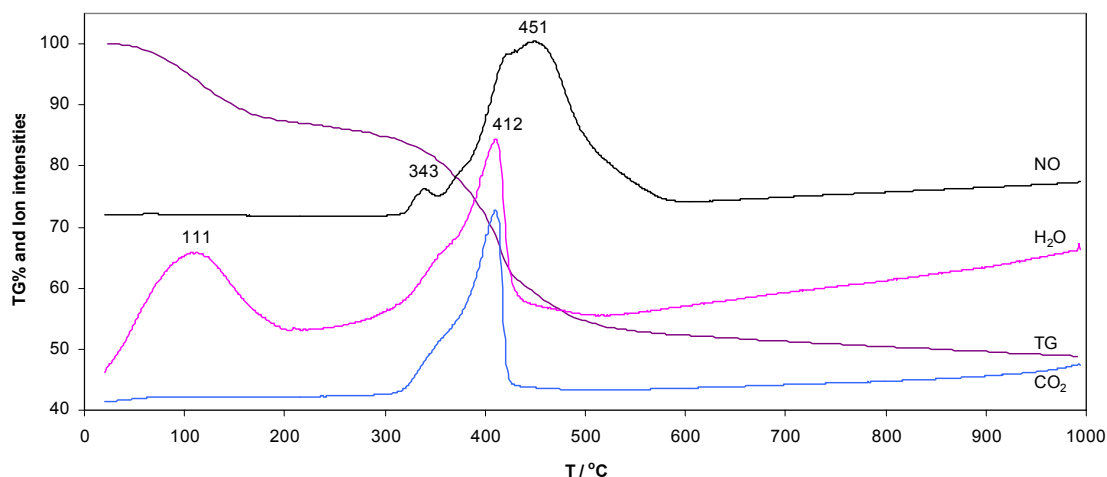


Fig. 4. TGA-MS pattern of NO_3 -hydrotalcite.

The stability of the NO_3 -hydrotalcite (Fig. 4) is higher than that of the CO_3 -hydrotalcite (Fig. 3). Since some carbonate was taken up in the hydrotalcite structure during the synthesis as shown by the infrared spectrum a major loss of CO_2 is observed around 412°C . The dehydration in this case takes place as a single event over a large temperature range up to 200°C , while dehydroxylation and the associated loss of H_2O around 412°C . The interlayer nitrated decomposes to NO with a minor loss around 345°C followed by a major loss around 450°C . It seems that the presence of nitrate in the interlayer stabilizes the interlayer carbonate resulting in an increase in temperature of about 80°C before this carbonate is lost. So far, there is no clear explanation for the minor NO loss around 345°C . The presence of NaNO_3 as a cause can be excluded since NaNO_3 melts at a higher temperature and decomposition does not take place until 650°C .

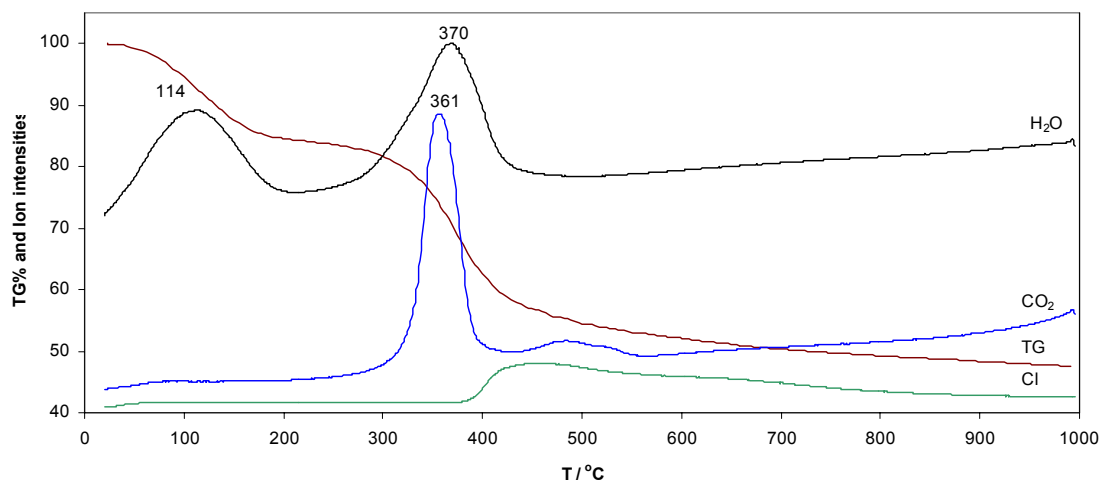


Fig. 5. TGA-MS patterns of Cl -hydrotalcite.

The Cl-hydrotalcite (Fig. 5) shows a similar behaviour for the H₂O loss (dehydration) as the NO₃-hydrotalcite, but Cl is lost over a larger and higher temperature range from 400 to 900°C. As with the nitrate the interlayer chloride anions seems to stabilize the interlayer carbonate as shown by the fact that after the major CO₂ loss around 360°C a second step is observed around 500°C coinciding with the major release of Cl₂. No HCl was detected.

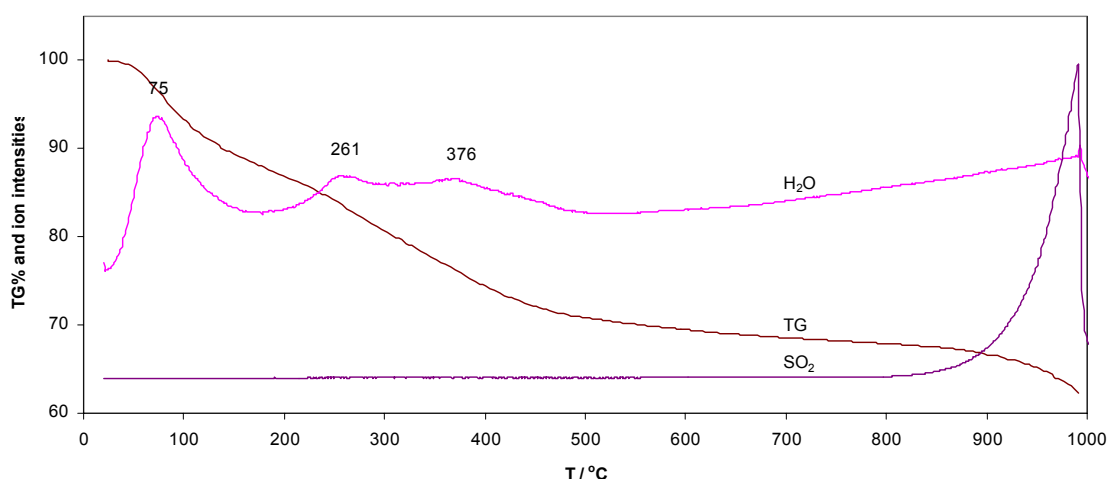


Fig. 6. TGA-MS pattern of SO₄-hydrotalcite.

Completely different is the thermal behaviour of SO₄- (Fig. 6) and ClO₄-hydrotalcites (Fig. 7). SO₄-hydrotalcite shows a gradual weight-loss due to dehydroxylation with two minor water peaks around 260 and 375°C, while the sulphate remains in the structure. The sulphate is not lost as SO₂ until a temperature of 850°C is reached. This may be interpreted as being due to the formation of separate phases of magnesium and aluminium sulphate upon dehydroxylation. The ClO₄-hydrotalcite shows a complex thermal behaviour with 2 steps of water loss around 375 and 440°C, where the second step is accompanied by the loss of O₂.

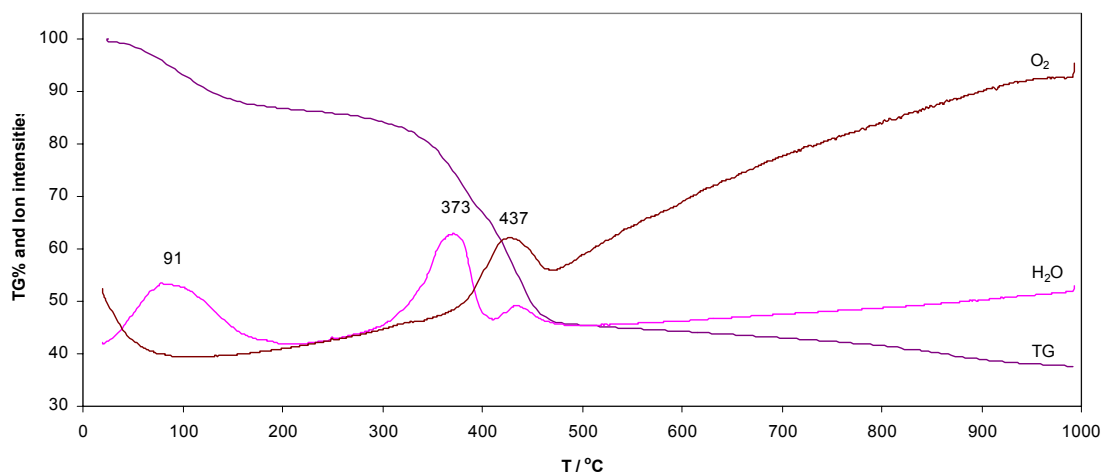


Fig. 7. TGA-MS pattern of ClO₄-hydrotalcite.

REFERENCES

- Bish, D.L. (1980) Anion-exchange in takovite: applications to other hydroxide minerals. *Bulletin de Mineralogie*, 103, 170-175.
- Brindley, G.W. and Kikkawa, S. (1979) A crystal-chemical study of Mg,Al and Ni,Al hydroxy-perchlorates and hydroxy-carbonates. *American Mineralogist*, 64, 836.
- Brindley, G.W. and Kikkawa, S. (1980) Thermal behavior of hydrotalcite and of anion exchanged forms of hydrotalcite. *Clays and Clay Minerals*, 28, 87-91.
- Hickey, L., Kloprogge, J.T. and Frost, R.L. (2000) The effects of various hydrothermal treatments on Mg/Al - hydrotalcites. *Journal of Materials Science*, 35, 4347-4355.
- Kloprogge, J.T. and Frost, R.L. (1999) Fourier Transform Infrared and Raman spectroscopic study of the local structure of Mg, Ni and Co - hydrotalcites. *Journal of Solid State Chemistry*, 146, 506-515.
- Kloprogge, J.T., Wharton, D. and Frost, R.L. (2000) Raman and infrared spectroscopy of interlayer CO_3^{2-} , NO_3^- , SO_4^{2-} and ClO_4^- in hydrotalcites. ICORS 2000, p. 96, Beijing, China.
- Kloprogge, J.T., Wharton, D., Hickey, L. and Frost, R.L. (2002) Infrared and Raman study of interlayer anions CO_3^{2-} , NO_3^- , SO_4^{2-} and ClO_4^- in Mg/Al-hydrotalcite. *American Mineralogist*, 87, 623-629.
- Marino, O. and Mascolo, G. (1982) Thermal stability of MgAl double hydroxides modified by anionic exchange. *Thermochimica Acta*, 55, 377-383.
- Miyata, S. and Kumura, T. (1973) Synthesis of new hydrotalcite-like compounds and their physico-chemical properties. *Chemistry Letters*, 843-848.
- Miyata, S. and Okada, A. (1977) Synthesis of hydrotalcite-like compounds and their physico-chemical properties - the system Mg^{2+} - Al^{3+} - SO_4^{2-} and Mg^{2+} - Al^{3+} - CrO_4^{2-} . *Clays and Clay Minerals*, 25, 14-18.
- Sato, T., Wakabayashi, T. and Shimada, M. (1986) Adsorption of various anions by magnesium aluminium oxide ($\text{Mg}_{0.7}\text{Al}_{0.3}\text{O}_{1.15}$). *Industrial & Engineering Chemistry Product Research and Development*, 25, 89-92.
- Titulaer, M.K. (1993) Porous Structure and Particle Size of Silica and Hydrotalcite Catalyst Precursors, *Geologica Ultraiectina* 99, p. 268. Utrecht University, Utrecht, The Netherlands.
- Vaccari, A. (1998) Preparation and Catalytic properties of cationic and anionic clays. *Catalysis Today*, 41, 53-71.